ISSN 1027-5495. Functional Materials, 27, No.1 (2020), p. 224-229.
doi:https://doi.org/10.15407/fm27.01.224

Advanced detonation gun application for aluminum oxide coating

***K.V.Korytchenko*[1], *O.Y.Hichlo*[1], *I.O.Belousov*[1], *A.V.Mats*[2], *O.A.Repikhov*[2], *C.Senderowski*[3], *D.P.Dubinin*[4], *A.V.Tytarenko*[4]**

[1]National Technical University "Kharkiv Polytechnic of Institute", 2 Kyrpychova Str., 61002 Kharkiv, Ukraine
[2]National Science Center "Kharkiv Institute of Physics and Technology", 1 Akademicheskaya Str., 61108 Kharkiv, Ukraine
[3]University of Warmia and Mazury in Olsztyn, 2 M.Oczapowskiego Str., Olsztyn, Warmia and Mazury, Poland
[4]National University of Civil Defence of Ukraine, 94 Chernyshevska Str., 61023 Kharkiv, Ukraine

Received July 11, 2019

The results of an investigation of the thermal spraying of aluminum oxide coating using an advanced detonation gun are presented. The improvement of the gun consists in the pulse compression of a detonating gas charge in the tube before a start of detonation initiation. It allows feeding the gun by a mixture of propane with air, as a detonating gas, instead of a mixture of propane with oxygen. A stainless steel substrate was coated by Al_2O_3 using the developed pulse compression detonation gun. The adhesion and roughness of the coating are shown as a function of thickness. The results of electron microscopic investigation and microhardness measurements are presented.
Keywords: detonation gun, compressed mixture, thermal coating, aluminum oxide.

Представлены результаты исследования термического напыления покрытия из оксида алюминия с помощью усовершенствованной детонационной пушки. Усовершенствование пушки заключается в импульсном сжатии детонирующего газового заряда в трубе перед началом инициирования детонации. Это позволило использовать в качестве детонирующего газа смесь пропана с воздухом вместо смеси пропана с кислородом. Разработанной пульсирующей компрессионно-детонационной пушкой наносилось покрытие Al_2O_3 на подложку из нержавеющей стали. Приведены зависимости адгезии, шероховатости покрытия от толщины. Представлены результаты электронно-микроскопических исследований и измерения микротвердости.

Застосування удосконаленої детонаційної гармати для напилення покриттів з окисду алюмінію. *К.В.Коритченко, О.Ю.Хіхло, І.О.Бєлоусов, О.В.Мац, О.О.Репіхов, Ц.Сендеровський, Д.П.Дубінін, А.В.Титаренко.*

Представлено результати дослідження термічного нанесення покриття оксиду алюмінію за допомогою вдосконаленої детонаційної гармати. Удосконалення гармати полягає в імпульсному стисненні газового заряду, що детонує, у трубі перед початком ініціювання детонації. Це дозволило використовувати газову суміш пропану з повітрям як заряд, що детонує, замість суміші пропану з киснем. Розробленою пульсуючою компресійно-детонаційною гарматою наносилося покриття Al_2O_3 на підкладку з нержавіючої сталі. Наведено залежності адгезії, шорсткості покриття від товщини. Представлено результати електронно-мікроскопічних досліджень і вимірювання мікротвердості.

1. Introduction

A thermal spray coating technology is widely used to improve functional performance of parts of various equipments [1, 2]. Thermal spray coating is applied to protect the parts from wear, abrasion, corrosion, high temperatures, etc. [3]. The coating can be released by several different technologies such as high velocity oxygen-fuels (HVOF) spray, plasma spray, wire arc spray, flame spray, detonation spray and others. High quality of the coating is achieved by detonation spray technology [4]. But this technology is expensive [5].

The pulse compression detonation gun was designed recently to reduce expenses for the coating [6]. We start using a compressed mixture of propane with air instead of an uncompressed mixture of propane with oxygen in the gun. It causes the changes in a technological regime of the coating. Thus, it needs to investigate the parameters of the new detonation gun. It requires evaluating a quality of coating deposited by the designed gun. We applied aluminum oxide coating in the presented research.

2. Pulse compression detonation gun as advanced technique of detonation coating

As usual, a detonation gun [7] consists of a smooth tube with closed one end, systems of fuel and oxidizes supplying, an ignition system, a system of neutral gas blowing and a pulsed powder feeder (Fig. 1). A length of the detonation tube exceeds a deflagration to detonation transition length L_{DDT} to initiate detonation by a traditional spark plug. A diameter d_{DT} of the tube exceeds a detonation cell size λ to have a deflagration to detonation transition [8]. It was experimentally evaluated for the smooth tube that $L_{DDT} = 20–40d_{DT}$ [9]. Thus, detonation cell sizes influence on the inner diameter and the length of the detonation gun. According to experimental data [10], the cell size of stoichiometric fuel/air mixture is higher than the size of the corresponding fuel/oxygen mixture by similar thermodynamic conditions. For example, the cell size of propane/air mixture is over $\lambda = 50–75$ mm [9, 10] at normal temperature and pressure. For comparison, the cell size of propane/oxygen mixture exceeds $\lambda = 1–2$ mm [11]. It causes a growth in the detonation gun size when the fuel/air mixture is applied. An increased gun size leads to a restriction of frequency of spraying too. Moreover, an increased tube diameter leads to nonuniform coating. Thus, a traditional detonation gun fed by fuel/air mixture is inefficient.

A compression of fuel/oxidizer mixture leads to decrease in the detonation cell size [12]. But there is a problem to compress the mixture because the one tube end is open. The specific compression solution should be applied. The pulse compression detonation gun (PCD-gun) uses a phenomenon of a supersonic combustion where detonation inside a tube generates an impulse by compressing a reactive gas whose products expand rapidly at the open end [6]. A pulsed mixture compression at the closed end of the detonation tube is generated by a piston compressor in such a manner that the mass flow rate at the "closed" end of the tube exceeds the mass flow rate at the open end of the tube. This causes compression of the air-fuel mixture within the tube. Detonation is then initiated when the mixture is compressed.

A diagram of the PCD-gun is shown in Fig. 2. The device consists of a piston compressor (1) composed of a cylinder (2) and a piston (3), arrangement as shown. Reciprocating motion of the piston (3) is enabled by a crank mechanism (4), coupled with an external drive motor. The top of the cylinder (2) has the attached cylinder head (5) with an intake branch tube (6) and valve (7). The

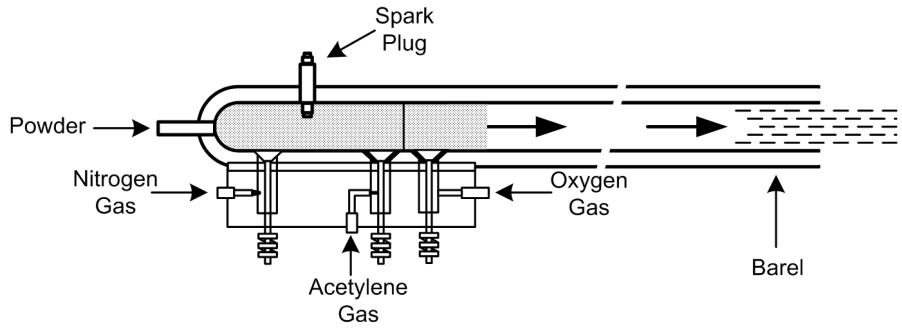

Fig. 1. Scheme of the traditional detonation gun [7].

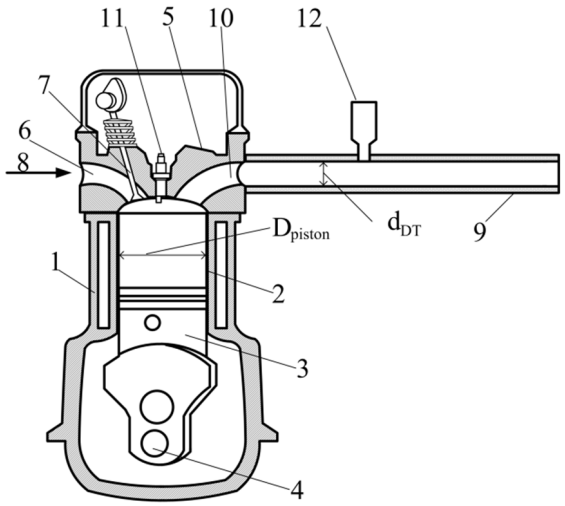

Fig. 2. Diagram of the PCD-gun: *1* — piston-type compressor; *2* — cylinder; *3* — piston; *4* — crank mechanism; *5* — head of the compressor; *6* — intake branch tube; *7* — valve; *8* — fuel feed system; *9* — barrel; *10* — branch tube; *11* — spark plug; *12* — powder feeder.

fuel-air feed system (8) is connected to the intake branch tube (6). The detonation tube-barrel (9) is connected to the cylinder (2) of the piston compressor (1) through an outlet branch tube (10) in the cylinder head (5). Forced ignition of the mixture is produced by a conventional automotive spark plug system (11). The powder is injected into the tube by a powder feeder (12). A special valve located in the branch tube (10) was used to avoid a backflow of combustion products during an intake stroke.

The inner diameter of the detonation tube was 20 mm. The length of the detonation tube was 1.37 m. The cylinder bore was 95 mm. The piston stroke was 105 mm. The compressor speed was 2700±100 rpm. A mixture of LPG with air was fed at 30±3 mg/cycle, which formed a fuel/air mixture close to stoichiometric composition in the piston compressor. Two piezoelectric pressure sensors, spaced 66 mm apart, were used to investigate the compression stroke and detonation process. The first pressure sensor was located near the cylinder head. The second sensor was located at the middle of the tube. Then we replaced the second sensor by a powder feeder to investigate the coating.

We measured the distance of the detonation initiation. The result of the pressure measurement is presented (Fig. 3). We observed a precompression Δp_1 and explosive combustion at the point of the fist sensor.

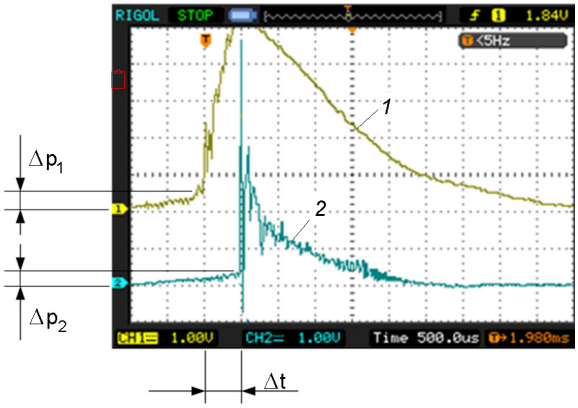

Fig. 3. Pressure behavior at the point of the first sensor (*1*) and at the point of the second sensor (*2*) during the detonation cycles; time resolution is 500 μs/div; pressure sensitivity is 8 bar/div.

We had the precompression Δp_2 and detonation at the point of the second sensor. We evaluated the average velocity of the combustion wave propagation between the sensors. The calculated average velocity was 1465±145 m/s. This confirms an extremely short deflagration-to-detonation transition length (shorter than 66 mm) within the PCD-gun. It also confirms a previous result, where the detonation was observed at the tube end while the tube length was $L_{DDT} = 66$ cm [13, 14]. These results suggest that such an increase in the detonation sensitivity of the air-fuel mixture due to the increased initial mixture pressure and temperature provides effective control of the deflagration to detonation transition process within the tube. Thus, the powder was accelerated by a detonation wave in the designed gun.

The specific compression technique allowed reducing the size of the detonation gun fed by the fuel/air mixture. Moreover, the frequency of spraying was increased in 2–3 times. For example, the frequency of the traditional detonation gun is about 1–10 Hz [7]. For comparison, the frequency of the PCD-gun exceeds 23 z. The temperature of detonation products significantly decreases when the fuel/air mixtures are used instead of fuel/oxygen mixtures. It influences on the detonation coating technology. So, we tested the advanced detonation gun starting from aluminum oxide coating.

3. Materials and research technique

We use the 08X18H10 type of stainless steel as a substrate. The steel samples had dimensions of 30×20×1 mm and 5×5×1 mm

(width×height×thickness). The distance between the tube end and the substrate was 150 mm. We obtained samples with coating thickness of 30 μm, 50 μm, and 70 μm.

The strength of adhesion of the coating was measured by the method of sclerometry of thin metal films [1]; the method is widely used for the study of various deposited materials. Measurements of adhesion properties of the coatings were carried out with loads on the indenter from 20 g to 220 g and the indenter speed of 0.2 mm/sec. We used the samples with sizes of 30×20 mm^2. Moreover, the "scratching" of the indenter began with the uncoated area of the samples, gradually moving to the area with the maximum thickness of the coating.

Scanning electron microscopy was used to investigate the surface of the coating [2]. Samples of 5×5 mm^2 size were studied using an electron microscope REM-106 at an accelerating voltage of 20 kV and a magnification of 500, 1500 and 3000 for each sample. Using PMT-3 microhardness tester, the values of maximum, minimum and average microhardness were measured. The surface roughness was measured with a stationary profilometer with an accuracy of 0.05 μm (ΔR_z = 3 %) along the sample length from the uncoated area to the center of the spot.

4. Results and discussion

The results of the adhesion investigation are presented in Fig. 4. We observed the maximum adhesion strength P_{max} = 47 MPa for a sample with the coating thickness δ = 30 μm. The average strength was <P> = 45.8 MPa for this sample. The maximum adhesion strength reduced to P_{max} = 32 MPa when the coating thickness grew to δ = 50 μm. The average strength was <P> = 29 MPa in this case. The measured strength was P_{max} = 28.6 MPa and the average strength was <P> = 23.3 MPa for a sample with δ = 70 μm. We have found that the measured value of the strength depends on the depth of the transition layer. We had a minimum strength when the depth of the transition layer was 2.5–10 μm. Further rise in the depth led to an increase in the strength of adhesion. But we observed a slight strength reduction near the boundary line between the coating and the substrate. The variation of the strength can be caused by porosity of the coating. It is worth to note that similar values of the adhesion strength were obtained when the "Prometey" detonation gun fed by fuel/oxygen mixtures was used for coating [15].

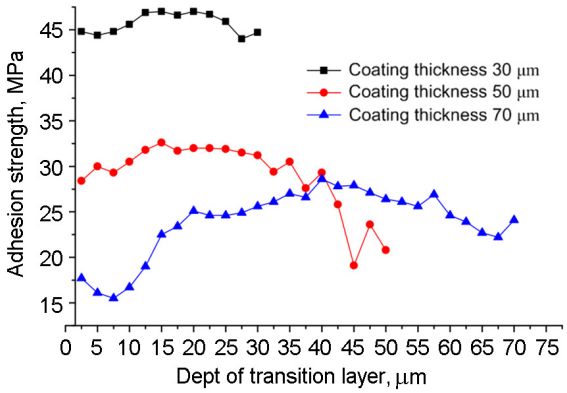

Fig. 4. Dependences of adhesion strength on the transition layer depth for samples with different coating thicknesses.

Table. Microhardness of samples with different coating thicknesses

	$H\mu_{av}$, MPa	$H\mu_{min}$, MPa	$H\mu_{max}$,MPa
δ = 30 μm	7500	6000	9000
δ = 50 μm	9750	8500	11000
δ = 70 μm	11000	9000	13000

Electron microscopic images of the coated samples are presented in Fig. 5. We observed complex surface-relief structures. The grains can be interpreted as an agglomerate of aluminum oxide powder particles which are partially melted. The contrast variation was used to evaluate the grain size. The maximum grain size was 10 μm. The sample with the coating of 70 μm had a higher contrast variation than the sample with the coating thickness of 30 μm. The grain size was reduced for thinner coatings.

The results of measurements of maximum, minimum and average microhardness for samples with coating thicknesses δ = 30 μ, δ = 50 μ, δ = 70 μm are presented in Table.

From the above data, it is possible to estimate the heterogeneity of the coating. It should be noted that the maximum value of microhardness is observed in the samples with coating thicknesses of 50 μm and 70 μm in the region of large grains.

The change of surface roughness along sample length is shown in Fig. 6. The surface roughness of the samples was measured with a stationary profilometer with an accu-

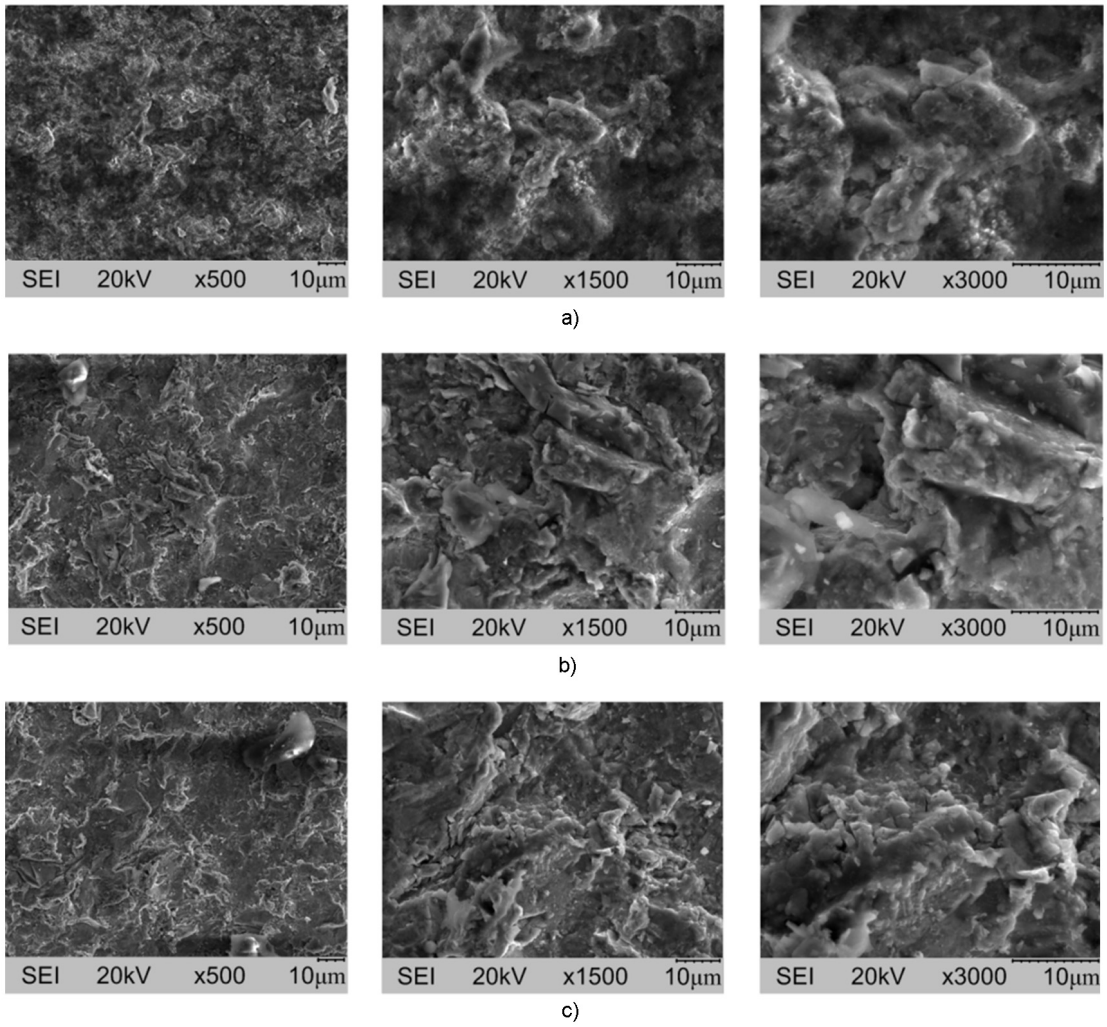

Fig. 5. Electron microscopic images of samples with different coating thicknesses δ at 500×, 1500× and 3000× magnifications: a) δ = 30 μm; b) δ = 50 μm; c) δ = 70 μm.

racy of 0.05 μm (ΔR_z = 3 %) along the sample length (30 mm) from the uncoated area to the center of the spot. The plots are divided into four areas: 1 — no coating, 2 — area with a coating thickness, average over the sample, 3 — area with the greatest thickness of the coating "halo" around the center of the spot, 4 — center of the spot where a coating thickness is average. The oxide film was detected at the "substrate-coating" boundary using XRD analysis.

5. Conclusions

A short length of deflagration to detonation transition in the pulse compression detonation gun fed by the propane/air mixture was experimentally confirmed. The length did not exceed 66 mm when the tube inner diameter was 20 mm.

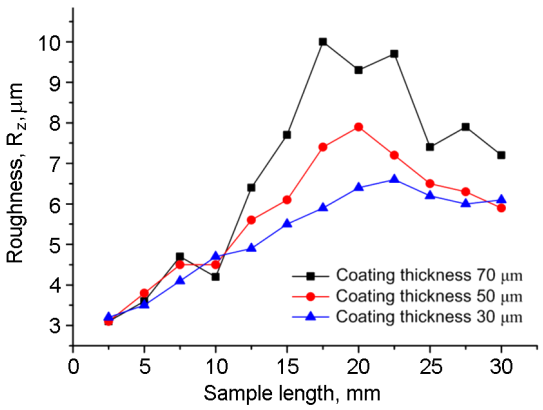

Fig. 6. Roughness of samples with coating thicknesses δ = 30 μm, δ = 50 μm, and δ = 70 μm.

Preliminary experimental results have demonstrated ability to use the pulse compression detonation gun for aluminum oxide coating. The adhesion strength was in the range from 15 MPa to 45 MPa depending on the transition layer depth and the coating thickness. The measured roughness of samples varied from 3 μm to 10 μm.

The investigations of coatings obtained by the pulse compression detonation gun should be continued for varies types of coating materials and the coating regimes. *Acknowledgements*. This study was supported by National Science Centre, Poland, Research Project No 2015/19/B/ST8/02000.

References

1. A.J.Panas, C.Senderowski, B.Fikus, *Thermochim Acta*, 676 (2019). https://doi.org/10.1016/j.tca.2019.04.009
2. B.Fikus, C.Senderowski, A.J.Panas, *J. Thermal Spray Technology*, **28**, 3 (2019). https://doi.org/10.1007/s11666-019-00836-6
3. M.Kutz, Handbook of Environmental Degradation of Materials, A.William (2018). https://doi.org/10.1016/C2016-0-02081-8
4. G.Sundararajan, D.Srinivasa Rao, G.Sivakumar et al., Detonation Spray Coatings, Springer, MA (2013). https://doi.org/10.1007/978-0-387-92897-5_704
5. K.N.Balan, B.R.Ramesh Bapu, *Procedia Engineer*, 38 (2012). https://doi.org/10.1016/j.proeng.2012.06.078
6. WO Patent 2019045669 (2019).
7. L.Singh, V.Chawla, J.S.Grewal1, *J. Minerals .Mater. Charact. .Engin.*, 11, (2012). *doi:10.4236/ jmmce.2012.113019*
8. W.Breitung, C.Chan, S.Dorofeev et al., Flame Acceleration and Deflagration-to-detonation Transition in Nuclear Safety, OECD Nuclear Energy Agency (2000).
9. M.A.Nettleton, Gaseous Detonations: their Nature, Effects and Control, Chapman and Hall (1987). https://doi.org/10.1002/ep.670060311.
10. R.Driscoll, Master of Science in the School of Aerospace Systems of the College of Engineering and Applied Sciences (2013).
11. B.A.Rankin, S.W.Theuerkauf, F.R.Schauer, Performance, Application, and Analysis of Rotating Detonation Engine Technologies, Preprint (2015).
12. B Zhang, H.Dick Ng, R.Mevelet et al., *Intern. J. Hydrogen Energy*, **36**, (2012). https://doi.org/10.1016/j.ijhydene. 2011.01.175.
13. D.Dubinin, K.Korytchenko, A.Lisnyak et al., *Eastern-European J.Enterprise Technol.*, **2**, 10 (2018). https://doi.org/ 10.15587/1729-4061.2018.127865
14. K.Korytchenko, Yu.Kysternyy, O.Sakun, in: 26th ICDERS Conf., Boston, MA, USA (2017), p.127.
15. A.Vinogradov, Degree Programme in Mechanical Engineering and Production Technology (2015).